Available online at www.sciencedirect.com

ScienceDirect

Geochimica et Cosmochimica Acta 133 (2014) 325–339

Geochimica et Cosmochimica Acta

www.elsevier.com/locate/gca

The influence of salinity on D/H fractionation in dinosterol and brassicasterol from globally distributed saline and hypersaline lakes

Daniel B. Nelson *, Julian P. Sachs

University of Washington, School of Oceanography, Box 355351, Seattle, WA 98195, USA

Received 2 July 2013; accepted in revised form 4 March 2014; Available online 14 March 2014

Abstract

Salinity, growth rate, growth stage, nutrient limitation and temperature have all been shown to influence the magnitude of D/H fractionation in algal lipids through laboratory and field studies. Of these factors, salinity has been studied most extensively in the field, but to date all such investigations have focused on transect studies within specific and isolated environments. Here we test the relationship between salinity and the magnitude of D/H fractionation in algal lipids through paired analyses of sedimentary and particulate lipid and water hydrogen isotope values at a wide range of continental and coastal lake sites spanning salinities from 0 to 117 ppt. Our results demonstrate broad consistency between D/H fractionations in dinosterol and brassicasterol with those obtained from previous work, with salinity changes of 1 ppt resulting in lipid δD changes of 0.7–1‰. Although our results also show variability in D/H fractionation between sites that is not related to salinity, the fact that any relationship emerges above the influences of other factors suggests that the salinity effect is dominant for some lipids in the majority of saline to hypersaline environments. This improved understanding of D/H fractionation in dinosterol and brassicasterol synthesis supports the use of these compounds as paleohydrologic indicators. When combined with D/H measurements from a second lipid or oxygen isotope measurements from carbonate, quantitative reconstructions of salinity and lake water isotope changes are possible. Extending the number of algal lipids within which a consistent relationship between D/H fractionation and salinity has been identified also supports the notion that the relationship is widespread among unicellular photoautotrophs.

1. INTRODUCTION

The hydrogen isotopic composition of organic compounds offers unique insights on a variety of processes in the natural world, including biosynthetic pathways and paleohydrology. Paleohydrologic applications target organic compounds that are well preserved in sediments and can be traced to a particular biologic source. But typical lipid extracts from sediments contain a diverse assortment of compounds that vary by environment and the significance of the hydrogen isotope signal preserved in most compounds is only beginning to be understood. Calibration efforts have routinely demonstrated that in most environments the hydrogen isotopic composition, or D/H ratio (D and H stand for deuterium and protium, respectively) of lipids from terrestrial and aquatic autotrophic organisms tracks the hydrogen isotopic composition of environmental water (Sachse et al., 2012 for a review). However, sediment based records that seek to exploit this relationship through measurements of changing biomarker hydrogen isotope values over time are limited to qualitative interpretations due to an incomplete understanding of the degree to which

* Corresponding author. Tel.: +1 206 685 9879.
E-mail address: dbnelson@uw.edu (D.B. Nelson).

http://dx.doi.org/10.1016/j.gca.2014.03.007
0016-7037/

various additional factors act to modulate the magnitude of isotopic fractionation between source water and lipid hydrogen isotope values. For higher plant lipids these include humidity, evapotranspiration rates, salinity, timing of leaf wax production, and vegetation assemblage (Smith and Freeman, 2006; Hou et al., 2008; Liu and Yang, 2008; Sachse et al., 2009; Yang et al., 2009; Polissar and Freeman, 2010; McInerney et al., 2011; Zhou et al., 2011; Douglas et al., 2012; Ladd and Sachs, 2012; Kahmen et al., 2013; Nelson et al., 2013; Tipple et al., 2013). Factors known to influence D/H fractionation in lipids from aquatic photoautotrophs include salinity, nitrogen-limited growth rate, growth phase, and temperature (Schouten et al., 2006; Zhang and Sachs, 2007; Sachse and Sachs, 2008; Wolhowe et al., 2009; Zhang et al., 2009; Sachs and Schwab, 2011; van der Meer et al., 2013).

While the variety of secondary effects on the hydrogen isotope signal preserved in lipids may be complex and numerous, there are also numerous lipids preserved in any given sediment sample, all of which incorporate hydrogen from the same external pool of environmental water. Since many lipids are essentially recording the same environmental signal, continued study of the secondary influences on hydrogen isotope fractionation in biomarkers should lead to improved paleohydrologic applications, either by making quantitative paleoprecipitation reconstructions possible through the use of multiple calibrated biomarkers, or at a minimum by helping to confirm that the most appropriate biomarkers are targeted for qualitative applications.

An increase in the salinity of environmental water has been shown to correlate with decreasing D/H fractionation (increasing α values; $\alpha = [D/H_{lipid}]/[D/H_{water}]$) for algal lipids in laboratory culture experiments (Schouten et al., 2006), and in field calibration studies (Sachse and Sachs, 2008; Sachs and Schwab, 2011). Sachs and Schwab (2011) observed that the relationship between dinosterol α values and salinity in the Chesapeake Bay displayed a near identical slope, but a different intercept, from the relationships observed for hydrocarbons from hypersaline ponds on Christmas Island (Sachse and Sachs, 2008). This result led to the suggestion that the influence of salinity on α values may be universal among unicellular photoautotrophs. Notably, these observations differed in magnitude, but not sign, from a series of batch culture experiments with *Emiliania huxleyi* and *Gephyrocapsa oceanica*, both marine haptophytes, whose alkenone α values were also shown to increase with increasing salinity (Schouten et al., 2006; van der Meer et al., 2013). However, alkenone α values from the Chesapeake Bay (Schwab and Sachs, 2011) and lakes in North America (Nelson and Sachs, 2014) showed no relationship with salinity. Recent analysis of a 60-year sediment record from a hypersaline lake in Mexico documented δD values of a 1,15-C_{32} diol thought to be produced by algae from the class Eustigmatophyta, that are inversely correlated with precipitation, and presumably salinity as well (Romero-Viana et al., 2013). Although δD values of water were not measured directly, the results strongly imply a decrease in D/H fractionation with decreasing salinity ($\delta D = [(D/H_{sample}/D/H_{standard}) - 1]$). The authors interpreted this relationship as a growth rate effect, and argued that increasing salinity in this system plays a key role in limiting carbon solubility leading to carbon limited growth rates during dry periods. If so, this would indicate that in certain environments such effects may be more important than salinity in determining the magnitude of D/H fractionation, or that the sensitivity of fractionation to salinity can be lipid- or organism-specific.

In the present study we sought to evaluate the relationship between $\alpha_{lipid\text{-}water}$ and salinity through paired analyses of δD_{water} values and δD_{lipid} values from surface sediments and suspended particles in saline and hypersaline lakes. The environments that we targeted encompassed salinities from 0 to 117 ppt, and δD_{water} values from $-81.1‰$ to $+13.2‰$ and span a latitudes from 1°S to 53°N (Fig. 1 and Table 1). By examining such a variety of aquatic systems we aimed to incorporate a wide range of algal species, growth rates, and temperatures, all of which have been identified as additional factors that can influence the magnitude of D/H fractionation during lipid synthesis (Schouten et al., 2006; Zhang and Sachs, 2007; Sachse and Sachs, 2008; Wolhowe et al., 2009; Zhang et al., 2009; Sachs and Schwab, 2011; Romero-Viana et al., 2013). At the scale of our sample set such competing factors should be uncorrelated with salinity, so this approach provides an effective means to evaluate its importance relative to other influences on the magnitude of D/H fractionation in the targeted compounds. We focused on D/H fractionation in dinosterol (4α, 23, 24-trimethyl-5α-cholest-22E-en-3β-ol) and brassicasterol (24-methyl cholest-5, 22-dien-3β-ol). By targeting two algal biomarkers we also hoped to evaluate whether δD values of sterols from separate classes of algae record similar environmental variability, and therefore whether any possible signal is unique or more common among algal sources.

Dinosterol is primarily produced by dinoflagellates, although it has also been shown to occur in some diatoms (Volkman et al., 1998; Volkman, 2003; Rampen et al., 2010). Dinosterol δD values have been the focus of both calibration (Sachs and Schwab, 2011), and paleoclimate studies (Sachs et al., 2009; Smittenberg et al., 2011). Brassicasterol is a commonly used diatom biomarker, and has been referred to as 'diatomsterol' although it has been reported in many algal classes (Volkman et al., 1998; Volkman, 2003; Rampen et al., 2010). Although applied extensively as a sedimentary biomarker for diatoms, it is also found in other plant sources including some plant oils (Zarrouk et al., 2009). While this may add to the complexity associated with interpreting a sedimentary record using δD values of this compound, it should at least be exclusively reflective of photoautotrophic sources and the dominant source should still be from diatoms in aquatic environments. To our knowledge, this is the first report of brassicasterol δD values so the sensitivity to climate variability is presently untested.

Dinosterol and brassicasterol were selected for study due to their relatively high degree of source specificity and widespread distribution among the lacustrine environments that were sampled. We report only on those locations where these compounds were found (Fig. 1 and Table 1), which

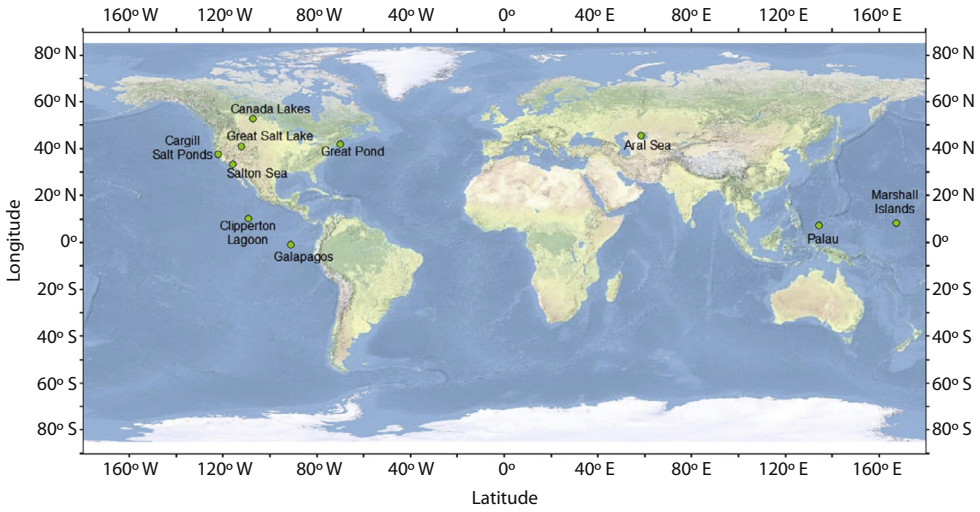

Fig. 1. Base map showing the collection locations for all samples used in the present study. The Canadian, Cargill, Galapagos, and Palau lakes, as well as the Aral Sea sites each contained more than one sample location (Table 1), but these regions are represented by only one point on the map for clarity.

was approximately 37% of sites for dinosterol and 72% of sites for brassicasterol. A complete list of sites, including those where neither compound was found, is available in the Electronic Annex. In addition to our measurements we include all published dinosterol data from contemporary samples where D/H fractionation could be calculated (Sauer et al., 2001; Sachs and Schwab, 2011; Smittenberg et al., 2011).

2. METHODS

2.1. Sediment and water sampling

Samples discussed in the present study are divided into broad categories based on provenance and sample collection techniques. Surface sediment samples from tropical Pacific island lakes were taken from sediment cores at each site, recovered with either a universal corer (Aquatic Research, Hope, ID), or a modified Livingstone-type corer (Geocore, Columbus, OH). Sediment cores were sectioned in the field at 1 cm intervals. Suspended particle samples were collected from the water column at sites in the tropical Pacific by filtering lake water through 0.7 μm glass fiber filters (Whatman GF/F). Surface sediment samples from the Cargill salt ponds were collected from the Cargill Salt Works facility in the San Francisco Bay area in June of 2008 using a hand sampler deployed in shallow water. Sediments from remaining continental interior lakes were sampled by Van Veen dredge-type recovery or by hand sampler deployed in shallow water. Sediment samples collected by dredge typically resulted in the recovery of large volumes of material from sediment depths approaching 20 cm. Many of the sediment samples from the continental interior lake sites were sampled during the fieldwork described in Bowman and Sachs (2008). All sediment and particle samples were frozen at −20 °C shortly after collection.

Lake water conductivity was measured at most sites at the time of sampling with a hand held conductivity sensor, and salinities were calculated based on the relationship between conductivity and salinity in seawater. The specific sensor type used was either from Hydrolab (Hach, Loveland, CO), YSI (YSI Inc., Yellow Springs, OH), or Eureka (Geo Scientific Ltd., Vancouver, BC), depending on when the samples were collected. Given the routine nature of conductivity measurements and the accuracy and precision of commercially available sensors it is unlikely the sensor type used at any particular site is an issue. In all cases, lake water samples were collected for δD_{water} measurements in screw cap glass vials that were sealed with electrical tape on site at the time of sediment recovery.

2.2. δD_{water} measurements

Two separate measurement techniques were used to measure δD_{water} values depending on the time of collection and processing. Some were determined at the University of Washington using a Thermal Conversion Elemental Analyzer (TCEA) interfaced with a Delta V Plus Isotope Ratio Mass Spectrometer (IRMS) (Thermo Scientific, Waltham, MA). The H_3^+ factor was evaluated at the beginning of each sample sequence and was stable between 5 and 6 ppm/mV over the duration of the measurements (Sessions et al., 2001). Each sample was analyzed over six consecutive injections with the first three omitted from reported values due to memory effects from the previous sample. δD values were determined in the Isodat 2.0 software platform relative to monitoring gas hydrogen, and then post-processed using measured values of two standards (0‰, and −189.5‰) analyzed in the same sequence to reference the data to the VSMOW scale (Vienna Standard Mean Ocean Water). Additional water samples were analyzed at the University of Hawaii in the laboratory of Dr. Brian Popp by Cavity

Table 1
Location and salinity information for the lakes used in this study. Salinity error estimates are based on inferred historical changes (see text; Electronic Annex). Sample coordinates, water depth from which sample was collected, and sampling technique is also given.

Site	Salinity (ppt)	Estimated salinity error +	Estimated salinity error -	Latitude (decimal degrees)		Longitude (decimal degrees)		Sample water depth (m)	Sampling technique
Tropical Pacific Island lakes									
Suspended particles									
Poza del Diablo, Galápagos	7	0	0	0.953	S	90.991	W	Surface	Filter
Poza Escondida, Galápagos	33	0	0	0.959	S	90.993	W	Surface	Filter
Flamingo Lagoon, Galápagos	40	0	0	1.228	S	90.429	W	Surface	Filter
Poza Verdes, Galápagos	43	0	0	0.959	S	90.991	W	Surface	Filter
Surface sediments									
El Junco Lake, Galápagos	0	0	0	0.896	S	89.480	W	6	Core top
Clipperton Lagoon	5	5	5	10.304	N	109.219	W	32	Core top
Poza del Diablo, Galápagos	7	5	5	0.953	S	90.991	W	1	Core top
Clear Lake, Palau	22	5	5	7.153	N	134.359	E	15	Core top
Lib Pond, Marshall Islands	27	5	5	8.315	N	167.381	E	3	Core top
Spooky Lake, Palau	27	5	5	7.152	N	134.363	E	13	Core top
Poza Escondida, Galápagos	33	5	5	0.959	S	90.993	W	1.5	Core top
Flamingo Lagoon, Galápagos	40	5	5	1.228	S	90.429	W	0.5	Core top
Poza Verdes, Galápagos	43	5	5	0.959	S	90.991	W	4	Core top
Continental lakes									
Great Pond, USA	0	0	0	41.973	N	70.031	W	Unknown	Unknown
Small Aral Sea	21	9	9	45.500	N	58.500	E	Unknown	Unknown
Redberry Lake, Canada	20	15	15	52.707	N	107.208	W	10	Dredge-type
Manito Lake, Canada	24	10	10	52.788	N	109.777	W	6	Dredge-type
Salton Sea, USA	35	5	10	33.300	N	115.800	W	13	Dredge-type
Big Quill Lake, Canada	43	20	20	51.782	N	104.323	W	3.3	Dredge-type
Chappice Lake, Canada	49	57	15	50.163	N	110.370	W	<1	Hand sampler
Large Aral Sea	55	25	25	45.500	N	59.500	E	Unknown	Unknown
Great Salt Lake (South), USA	117	17	34	41.061	N	112.238	W	1.3	Dredge-type
Cargill Salt Ponds, San Francisco Bay, California, USA									
Cargill Salt Pond 2	32	10	10	37.563	N	122.129	W	<1	Hand sampler
Cargill Salt Pond 3	40	10	10	37.546	N	122.093	W	<1	Hand sampler
Cargill Salt Pond 1	58	10	10	37.566	N	122.109	W	<1	Hand sampler
Cargill Salt Pond 12	78	10	10	37.477	N	122.026	W	<1	Hand sampler
Cargill Salt Pond 7	117	10	10	37.512	N	122.109	W	<1	Hand sampler

Ring Down Spectroscopy (CRDS) (Picarro, Inc., Santa Clara, CA), and are also reported in δD notation. Average analytical precision for all water samples was less than 1‰, but individual standard deviations of replicate analyses were calculated for each (Table 2).

2.3. Lipid extraction, saponification and column chromatography

Sediment samples were freeze dried and extracted in a 9:1 mixture of dichloromethane (DCM) and methanol (MeOH) on an accelerated solvent extractor (ASE) Dionex 200 operated at 100 °C and 1500 psi with three five-minute static phases. Excess solvent was evaporated under N_2 from the total lipid extract (TLE) on a Turbo-vap system (Caliper, Hopkinton, MA, USA). Subsequent TLE purification methods varied slightly between samples depending on the number of additional compounds that were targeted for other applications. These are described below in detail, but generally, TLEs were saponified, then separated into neutral and acid fractions using aminopropyl silica gel (NH_2) columns, and the neutral fraction was then separated into hydrocarbon, ketone/ester, alcohol, and polar fractions using silica gel columns. Some of these steps were omitted when the complexity of the sample matrix permitted less rigorous purification protocols.

Saponifications were performed by reacting the TLE with 1 N potassium hydroxide (KOH) in MeOH and Nanopure water (Barnstead nanopure infinity water system) at 70 °C overnight. The saponified TLE was then acidified to pH ~2 with HCl and recovered from the aqueous MeOH using a series of hexane liquid–liquid extractions. The hexane was then rinsed once with Nanopure water and dried over sodium sulfate.

Neutral and acid compounds in the saponified TLE were separated from each other using 0.5 g of 5% aminopropyl silica gel (Supelco/Sigma Aldrich, St. Louis, MO, USA, 45 μm, 60 Å, Part # 5-7205) in hand packed glass solid phase extraction (SPE)-type columns. Neutral compounds were eluted with 8 mL of DCM/isopropyl alcohol (IPA) (3:1), acids were eluted with 6 mL of 4% acetic acid in diethyl ether, and a polar fraction was eluted with 6 mL MeOH. Neutral fractions or TLEs were further separated into class fractions using the same type of glass hand packed column with 1 g of silica gel 60 (5% deactivated by weight; EMD chemicals, Rockland, MA, USA, 35–75 μm, 60 Å). Hydrocarbon fractions were eluted with 10 mL of hexane, ketones/esters with 6 mL DCM/hexane (1:1), alcohols with 8 mL ethyl acetate (EtOAc)/hexane (1:4), followed by a polar fraction with 6 mL methanol.

2.4. HPLC–MS purification of dinosterol and brassicasterol

HPLC–MS purifications of initial dinosterol samples used in this study were performed using the methods described in Atwood and Sachs (2012). Briefly, alcohol fractions from silica gel columns were injected on an Agilent 1100 series HPLC using an Agilent ZORBAX Eclipse XDB C_{18} column (4.6 mm × 250 mm × 5 μm) equipped with matching guard column operated at a constant temperature of 30 °C. Dinosterol was eluted with 5% MeOH in water at a flow rate of 1.5 mL/min (Atwood and Sachs, 2012). HPLC-purified dinosterol was then acetylated at 70 °C for 30 min in a mixture of 20 μL acetic anhydride and 20 μL pyridine. No underivatized dinosterol was detected following this acetylation procedure, ensuring the efficacy of the method. This purification procedure was modified during the course of the present study in favor of a more streamlined approach, which also enabled the concurrent purification of brassicasterol (Nelson and Sachs, 2013). For these samples, alcohol fractions from silica gel, or neutral fractions from aminopropyl columns were acetylated as described above prior to injection on the HPLC. The same HPLC configuration was used, but eluting acetylated-brassicasterol and -dinosterol required a mobile phase composition of 5% MeOH, 10% EtOAc, and 85% acetonitrile (ACN).

2.5. Gas chromatography–mass spectrometry

At each purification stage and prior to hydrogen isotope analysis, sample aliquots were analyzed by gas chromatography–mass spectrometry (GC–MS) to identify compounds of interest, assess the efficacy of separation procedures, and to determine subsequent handling steps. Samples were injected in splitless mode at 300 °C using helium carrier gas at 1.5 mL/min on an Agilent 6890N GC with 5975 inert mass selective detector. Optimal sterol GC separation was achieved with an Agilent (formerly Varian) VF-17ms column (60 m × 0.32 mm × 0.25 μm). Initial sample screening was performed with an oven temperature program that began at 110 °C for 3 min after sample injection, then increased to 170 °C at 15 °C/min, then to 325 °C at 5 °C/min where it was held for 24 min. For purified dinosterol and brassicasterol samples the GC oven was held at an initial temperature of 120 °C for 10 min, then increased to 260 °C at 20 °C/min, then to 300 °C at 1 °C/min, then to 325 °C at 20 °C/min and held for 8 min. All samples were run in full scan mode (*m/z* 50–700). Sample dilution required for isotope analysis was determined by quantification estimates based on the relative areas of unknown peaks to that of a 5α-cholestane internal standard of known concentration that was added to each sample prior to GC–MS analysis.

2.6. Gas chromatography–isotope ratio mass spectrometry

Purified dinosterol and brassicasterol δD values were measured by gas chromatography–isotope ratio mass spectrometry (GC–IRMS) using a Thermo Delta V Plus isotope ratio mass spectrometer and Thermo Trace GC Ultra coupled to a gas chromatography combustion/thermal conversion interface III. Samples were injected in splitless mode at 330 °C using helium carrier gas at 1.5 mL/min. The GC was equipped with either an identical column to the GC–MS, or a similar VF-17ms with slightly narrower diameter (60 m × 0.25 mm × 0.25 μm). The GC–IRMS oven program was identical to the GC–MS program for purified sterols with the exception of the initial oven temperature and hold time of 120 °C for 2 min. GC column effluent

Table 2
All measured and compiled salinity, δD_{water}, $\delta D_{dinosterol}$, $\alpha_{dinosterol\text{-}water}$, $\delta D_{brassicasterol}$ and $\alpha_{brassicasterol\text{-}water}$ data. Uncertainties for lipid and water isotope measurements reported in this table reflect the analytical uncertainty only, and do not incorporate the inferred historic changes in δD_{water} that were used to produce the error bars in Figs. 2–5. Uncertainties for salinity are based on historical changes in at continental interior sites, and probable variability at other locations (see text).

Site	Salinity (ppt)	Estimated salinity error +	Estimated salinity error −	δD-water (‰)	σ (‰)	δD-dino (‰)	σ (‰)	*n*	$\alpha_{dino\text{-}water}$	σ	δD-brass (‰)	σ (‰)	*n*	$\alpha_{brass\text{-}water}$	σ
Tropical Pacific Island lakes															
Suspended particles															
Poza del Diablo, Galápagos	7	0	0	13.2	0.6	−250	4	3	0.740	0.004	−263	2	4	0.728	0.002
Poza Escondida, Galápagos	33	0	0	4.5	0.6						−237	10	1	0.760	0.010
Flamingo Lagoon, Galápagos	40	0	0	5.5	0.5						−241	3	3	0.755	0.003
Poza Verdes, Galápagos	43	0	0	10.5	0.3						−240	6	2	0.753	0.006
Surface sediments															
El Junco Lake, Galápagos[a]	0	0	0	7.66	1.0	−256	5		0.739	0.005					
Clipperton Lagoon[b]	5	5	5	0.04	1.1	−307	5		0.693	0.005					
Poza del Diablo, Galápagos	7	5	5	13.2	0.6	−263	4	3	0.727	0.004					
Clear Lake, Palau[c]	22	5	5	−12.1	1.0	−280	5		0.726	0.005					
Lib Pond, Marshall Islands	27	5	5	3.0	0.4	−277	3	2	0.720	0.003					
Spooky Lake, Palau[d]	27	5	5	−7.6	1.0	−291	4	5	0.718	0.004					
Poza Escondida, Galápagos	33	5	5	4.5	0.6	−292	3	3	0.705	0.003	−228	4	3	0.768	0.004
Flamingo Lagoon, Galápagos	40	5	5	5.5	0.5	−268	4	2	0.728	0.004					
Poza Verdes, Galápagos	43	5	5	10.5	0.3	−261	4	3	0.732	0.004					
Continental lakes															
Great Pond, USA[e]	0	0	0	−24	2.0	−222	6		0.797	0.006					
Small Aral Sea	21	9	9	3.6	0.7	−316	3	2	0.682	0.003					
Redberry Lake, Canada	20	15	15	−81.1	1.2	−372	9	5	0.684	0.010	−322	11	2	0.737	0.012
Manito Lake, Canada	24	10	10	−78.5	0.6						−328	3	3	0.729	0.003
Salton Sea, USA	35	5	10	−25.0	1.0	−323	4	2	0.695	0.004					
Big Quill Lake, Canada	43	20	20	−99.7	0.2						−301	3	4	0.776	0.003
Chappice Lake, Canada	49	57	15	−75.2	0.6						−259	5	2	0.802	0.005
Large Aral Sea	55	25	25	−8.9	0.3	−281	3	5	0.726	0.003					
Great Salt Lake (South), USA	117	17	34	−60.7	1.2	−269	5	2	0.778	0.006	−246	1	3	0.803	0.002
Cargill Salt Ponds, San Francisco Bay, California, USA															
Cargill Salt Pond 2	32	10	10	−3.0	0.4	−295	10	1	0.707	0.010					
Cargill Salt Pond 3	40	10	10	6.3	0.4	−310	8	3	0.686	0.008	−216	5	4	0.779	0.005
Cargill Salt Pond 1	58	10	10	−7.3	0.4	−271	10	2	0.734	0.010	−231	3	3	0.775	0.003
Cargill Salt Pond 12	78	10	10	7.2	0.4	−265	10	1	0.730	0.010	−193	10	1	0.801	0.010
Cargill Salt Pond 7	117	10	10	20.5	0.4						−169	3	2	0.814	0.003

[a] Provided by A. Atwood.
[b] Provided by I. Mügler.
[c] Provided by J. Richey.
[d] Smittenberg et al. (2011).
[e] Sauer et al. (2001).

was pyrolized in the thermal conversion interface to convert organic column effluents to H_2 gas prior to introduction to the mass spectrometer. The H_3^+ factor was measured prior to every sample sequence (Sessions et al., 2001), and was stable and less than 5 ppm/mV.

All samples were analyzed with a mix of co-injection standards of known isotopic composition, which included a combination of nC$_{21}$, nC$_{23}$, nC$_{28}$, nC$_{32}$ and nC$_{34}$ alkanes (standards from Arndt Schimmelmann at Indiana University, Bloomington, IN, USA). Most samples were also analyzed in sequences that included an external standard with nC$_{26}$, nC$_{38}$, and nC$_{41}$ alkanes (standards from Arndt Schimmelmann at Indiana University, Bloomington, IN, USA). Initial isotopic evaluations of all peaks were performed within the Isodat 2.0 software relative to a calibrated reference gas. Secondary corrections were performed based on the regression of Isodat-reported δD values of n-alkane standards and their accepted values in order to maintain similar treatments of samples and standards, as well as to correct for potential scale compression or stretching as a result of the one-point referencing to VSMOW performed by the Isodat software. Most samples were analyzed at least three times over at least two separate sample sequences on different days, and measurement precision calculated as the standard deviation of multiple analyses was typically 4–6‰. For some samples only one injection was possible so uncertainties of 10‰ were assigned, which is near the maximum error reported for any sample with multiple injections. Peak areas less than 15 V·s were below the cutoff identified on this GC–IRMS to avoid size dependent δD effects, and were not considered (Polissar et al., 2009).

The δD value of the acetic anhydride used to derivatize the dinosterol and brassicasterol samples was determined by using acetic anhydride of known isotopic composition (purchased from Arndt Schimmelmann at Indiana University, Bloomington, IN, USA) to acetylate samples of 1,4-dihydroxybenzene, and 1,3,5-trihydroxybenzene. The δD values for these phenols were then determined by a mass balance calculation based on the number of total hydrogen atoms per compound and the weighted δD value contribution of the hydrogen of known isotopic composition in the acetyl groups to the measured δD value. Additional phenol samples were then acetylated with the stock acetic anhydride used to acetylate the dinosterol and brassicasterol samples, and the δD value of the unknown acetic anhydride was also determined by a mass balance calculation using the mean measured δD values of the non-exchangeable hydrogen in the phenols. The calculated δD value of the stock acetic anhydride was then used to correct the measured δD values of acetylated dinosterol and brassicasterol samples for the δD value of the added hydrogen.

3. SAMPLE LOCATIONS AND SETTING

The sites comprising the present study were selected for the very large range of salinities and water δD values they encompass, and the diversity of limnologies, catchments, and ecologies they represent (Table 1). Unfortunately, many individual sites are also known to have experienced large changes in salinity over the past several decades, and likely changes in δD_{water} values. In cases where the sampling technique recovered sediment spanning the upper 10–20 cm, the measured δD value of either dinosterol or brassicasterol purified from these materials is unlikely to represent the salinity or δD_{water} values that were measured at the time of sample collection. In order to accommodate this non-analytical uncertainty we used either historical average values or seasonal ranges of variability in salinity or δD_{water} values to produce what are likely to be more accurate, less precise, and more realistic estimates than the measured values of those parameters. In the following section we describe these estimates in detail by sample site. The Cargill salt ponds and the tropical Pacific island surface sediment samples are unlikely to be impacted to the same degree because the sample collection techniques used at these sites penetrated only one to a few cm into the sediment. These materials are therefore more likely to reflect conditions of the past few years, which should also be more consistent with salinity and δD_{water} values measured at the time of sample collection.

3.1. Salinity

The preferred modern oceanographic method for determining the salinity of water is by measuring electrical conductivity and applying an empirically determined calibration equation to convert these values to salinity on the practical salinity scale (Fofonoff, 1985). This proxy measurement has proven accurate and reliable in seawater because the relative abundances of the major ions do not change with respect to one another. In continental interior lake settings this assumption is invalid, and salinity is often measured in g/L or ppt determined by alternate methods (Anati, 1999). Although g/L and ppt are not directly comparable owing to the influence of salinity and temperature on water density, in most cases in our sample set g/L and ppt values are virtually identical to within the uncertainty required for our purposes of $\sim \pm 5$ g/L or ppt (Bowman and Sachs, 2008). We therefore use these values interchangeably where appropriate unless otherwise specified. For the Cargill and tropical Pacific sites we use the salinity derived from conductivity measurements.

3.2. Historical salinity changes

Historical time series records of salinity were compiled for each continental interior lake site by assembling all available measurements. These time series were then used to calculate a time-weighted average salinity at each site (Electronic Annex). Where possible we also incorporated estimates of sedimentation rates to determine the appropriate time over which to determine the average salinity (S). In cases where sediment accumulation rates were not available, we estimated this parameter based on data from other lakes.

The Large and Small Aral Sea salinities were both 10 g/L in 1960, but by 1989 they had risen to 30 g/L due to diversion of inflowing waters, and by 2006 the large Aral Sea salinity was as high as 80 g/L while the Small Aral Sea salinity had decreased to 12 g/L due to a restoration project

(Micklin, 2007). Sedimentation rates in the Aral Sea over the past 1.3 m of deposition are estimated at 3 mm/yr (Nourgaliev et al., 2003). Although the known salinity changes in the Aral Sea have been large, the quantity of recovered material was relatively low as compared to other continental interior lakes (sample collected by Hedi Oberhänsli, Freie Universität Berlin), and likely encompasses only the most recent ~20 years of deposition or the upper ~5 cm of material. Given the large changes in salinity and lack of constraint on the depth of recovered material, we report our measurements using the 1989–2006 average salinity in the Large and Small Aral Seas, and use an uncertainty range to include the 1989 and 2006 extremes, or 55 ± 25 ppt and 21 ± 9 ppt, respectively.

The Salton Sea was formed in 1905–1907 by accidental flooding of the Colorado River. Following this event, more than 23 cm of sediment have accumulated at a rate of ~2.3 mm/yr, while over the same interval salinity increased from 0 to ~40 g/L by ~1930, and has remained relatively constant at these levels since that time (Schroeder et al., 2002). The dredged sample recovered from this site (sample collected by Robert Baskin, USGS) probably incorporated most of the lacustrine sediment package. We therefore use the mean 20th century value $S = 35$ ppt (+5, −10).

Manito and Redberry Lake salinities were less variable over the 20th century than the Salton or Aral Seas, and also benefit from extensive historical data (Hammer, 1978; Bowman and Sachs, 2008). We use the time-weighted average for each site, and symmetric uncertainty envelopes around these values that encompass most of the time series data since the samples were collected using a dredge. This results in salinity estimates of 24 ± 10 ppt for Manito Lake, and 20 ± 15 ppt for Redberry Lake. Using the same approach and data sources, we report our measurements from Big Quill Lake relative to time-weighted average salinity of 43 ± 20 ppt because 20th century variability was from 16 to 71 ppt (Hammer, 1978; Bowman and Sachs, 2008).

Chappice Lake absolute salinity was 163.6 ppt in 2007 (Bowman and Sachs, 2008). This is a more accurate indicator of salinity than conductivity estimates in lakes where the relative ion abundances differ significantly from seawater (Anati, 1999). Although conductivity-based salinity estimates, total dissolved solids (TDS), and absolute salinity measurements were determined at every site from the continental interior lakes described by Bowman and Sachs (2008), of the sites within that sample set discussed in the present study only Chappice Lake TDS and absolute salinity differed from one another significantly. In order to compare to the historical record of conductivity (Vance et al., 1993 and references therein), we use the ratio between absolute salinity and conductivity measured in 2007 (Bowman and Sachs, 2008) to convert the pre-1990 conductivity record to absolute salinity. Chappice Lake is known to have become significantly saltier after the installation of a nearby weir in 1976 that diverted inflow. Prior to this, available conductivity data are low (~18 mS/cm; 27 ppt) and show minimal variability (Vance et al., 1993). We therefore assume pre-weir conductivity prior to the 1950s in order to calculate a time-weighted 20th century average salinity value of 49 ppt. We assign uncertainties to this estimate at half the range between this value and the minimum and maximum extremes, or 49 (+57, −15) ppt.

The Great Salt Lake was divided into north and south sections after construction of a causeway in 1959 (Arnow and Stephens, 1990). Since the inception of the current southern section of the Great Salt Lake it has experienced large changes in salinity, ranging from 50 ppt in 1986 to 270 ppt in 1961 (Arnow and Stephens, 1990; USGS, 2013). Salinity in the north section was greater than 250 ppt until the mid-1980s, and has never decreased below 150 ppt (Arnow and Stephens, 1990; USGS, 2013). Dinosterol and brassicasterol were not found in the sediments from the northern section so we assume that all production in the south section occurred at salinities lower than 150 ppt after the basins were separated. After the causeway was constructed salinity steadily fell and crossed the 150 ppt threshold in approximately 1971. We therefore use the post-1971 time-weighted average salinity of 117 ppt, and include uncertainty estimates spanning half the range between this average value and the 50 ppt and 150 ppt extremes, or 117 (+17, −34) ppt.

We are unaware of extensive published records of historical salinity changes from the Cargill salt ponds or the tropical island lakes used in this study where conductivity-based salinity measurements were used, but we also note that these samples were collected from sediment cores, or with a hand-sampler, and therefore are more representative of the upper 1–2 cm of sediment than the continental interior lake samples. Nevertheless it is likely that the snapshot measurements of salinity do not capture the range of conditions under which the sediments were deposited. We attempt to address this by assigning uncertainties of ±10 ppt to each of the Cargill salinity values, and ±5 ppt to each of the tropical Pacific salinity values. While this approach may be somewhat arbitrary, it is still likely to be better than simply using the analytical error from the salinity measurement.

In all cases it is not clear that the average salinity of lake water as defined here is truly representative of the average conditions during biomarker formation represented in the sediment samples. Production of a particular compound may be more active under certain salinities as compared to others. More tightly constrained salinity values would provide opportunity for reducing the range of possible conditions during which the compounds were produced, and permit a more accurate determination of the influence of salinity on D/H fractionation. However, without such knowledge the use of large error bars to encompass a wide range of possible formation conditions is the most conservative approach.

3.3. Historical δD_{water} changes

As is the case for salinity of the lake waters at our sample sites, the δD_{water} values measured during the sample collection are unlikely to be representative of the average conditions that existed during deposition of the sediments. Unfortunately, extensive historic measurements of δD_{water} values are not available from any of the locations sampled. In order to provide some estimate of the variation of

δD_{water} values during the timespan of sterol sample production, we use the 2006 range from the Great Salt Lake of 15‰ (Nielson and Bowen, 2010). The seasonal variability should provide an indicator of the extent to which mean values might have been expected to vary over time at the continental interior lake sites. Since the values are poorly constrained, we conservatively double the 15‰ value from the Great Salt Lake and plot uncertainties using ±15‰ for all continental interior sites on figures showing δD_{water} and α values, but still report the analytical error of our measurements in Table 2.

An uncertainty of 30‰ for our continental interior site δD_{water} values is further supported through comparison with more detailed isotope hydrology and modeling work that has been performed on analogous lake systems using oxygen isotopes. Pyramid and Walker Lakes in Nevada, USA, are both sensitive to evaporation and have varied between closed and open hydrologic conditions over the 20th century (Benson and Paillet, 2002). In sensitivity experiments designed to evaluate the response of lake water to changes in freshwater input of up to 30% the modeled oxygen isotopic composition of lake water never varied by more than 4‰ (Benson and Paillet, 2002). Simulations of lake water changes over the 20th century that included four decadal-scale drought events also resulted in shifts that were never greater than 4‰ (Benson and Paillet, 2002). Using the equation for the global meteoric water line (Craig, 1961) to convert from oxygen this translates to a 32‰ hydrogen isotope-equivalent response, which is of similar magnitude to our assumed uncertainty. Another example comes from Castor Lake, a small closed-basin system in Washington State where isotope hydrology modeling experiments as well as sediment core carbonate oxygen isotope measurements have been completed (Nelson et al., 2011; Steinman et al., 2012). In these studies modeled lake water oxygen isotope changes in response to shifting mean temperature, precipitation and humidity were never larger than 4‰ (Steinman et al., 2012), and a 6,000-year record of carbonate oxygen isotope values that should primarily reflect lake water also never varied by more than 4‰ (Nelson et al., 2011), or 32‰ δD_{water}-equivalent. The approximate estimated δD_{water} response of these comparatively large and small volume continental interior lakes with sensitive hydrologic settings to changing conditions thus supports our application of a similar range of variability for the unconstrained changes in the lakes used in the present study. Although it is possible that the true uncertainties at our sites are asymmetric or smaller than the ranges that we use, it is unlikely based on comparisons to the analogous systems discussed above that they were much larger, so these estimates represent the best approximation that can be made given the information available.

High latitude sites as well as sites that are located far from the ocean typically display greater isotopic variability of precipitation than those from low latitudes or those located close to the sea (Rozanski et al., 1992). In addition, the coastal and tropical surface lake sediments that we used in this study were collected with techniques that resulted in limited recovery of material from sediments deeper than 5 cm at the Cargill sites, and virtually zero recovery of material from depths greater than 2 cm at the tropical Pacific sites. These samples are therefore likely to reflect conditions of the recent past and measured δD_{water} values. Accordingly, we use reduced uncertainty envelopes of ±10‰ for the Cargill sites and ±5‰ for the tropical Pacific sites.

4. RESULTS AND DISCUSSION

4.1. Salinity–δD_{water} relationships

In marine environments salinity values are highly correlated with δD values of seawater (Craig and Gordon, 1965), but for the continental saline lakes we sampled this relationship is inconsistent, and forms much of the motivation behind our chosen sample set (Fig. 2 and Table 2). By targeting sites that exhibit no relationship between salinity and δD_{water} values, we are able to reduce the potential for alternative factors that might be correlated with δD_{water} values to produce a non-causal correlation between α values and salinity.

4.2. D/H fractionation and salinity

We calculated slope, intercept and R^2 values between $\alpha_{lipid\text{-}water}$ values and salinity using standard methods, but this approach does not incorporate the large and non-uniform uncertainties associated with the properties of the lake water in this sample set. To address this, we also used a Monte Carlo (MC) approach by generating 10,000 sets of randomly selected salinity and δD_{water} values with distributions for each site that matched our historical estimates. We report the calculated slope, intercept, R^2, and P values, as well as the Monte Carlo slope, intercept, and R^2 values for comparison (Figs. 3 and 4). In cases where dinosterol or brassicasterol from both sediments and suspended particles were analyzed, only the suspended particle value is plotted and included in the regression of α values and

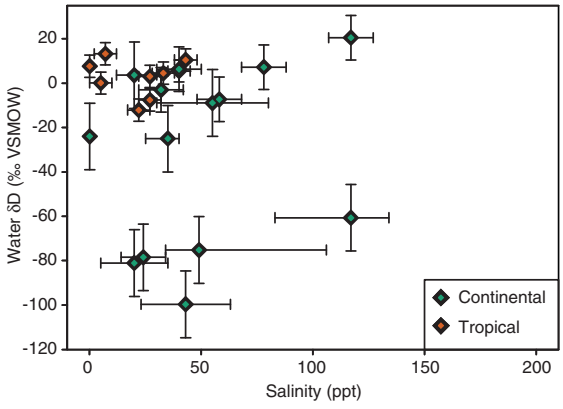

Fig. 2. Salinity vs. δD_{water} values from all sites. Salinity error bars are based on historical changes in salinity at continental interior sites, and probable variability at other locations (see text). Error bars for δD water values are estimated using seasonal variability as well as isotope hydrology model results and paleoclimate data from analogous systems as a guide (see text).

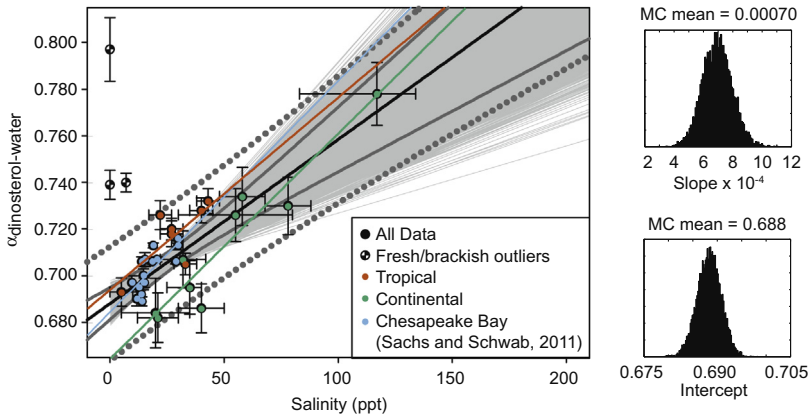

	N	slope	±	intercept	±	R^2	±	P
All Data	**32**	0.0007	0.0001	0.688	0.003	0.662	0.012	<0.0001
All Data - MC	**32**	0.0007	0.0001	0.688	0.003	0.577	0.091	-
Tropical	**7**	0.0008	0.0003	0.694	0.010	0.563	0.010	0.0521
Continental	**9**	0.0010	0.0001	0.665	0.007	0.901	0.011	<0.0001
Chesapeake Bay	**16**	0.0010	0.0002	0.685	0.004	0.572	0.006	0.0007

Fig. 3. Salinity vs. $\alpha_{dinosterol\text{-}water}$ (scatter plot). Error bars on each data point incorporate inferred historical changes in salinity and δD_{water} values in addition to the analytical uncertainty from the $\delta D_{dinosterol}$ measurement (see text). $\alpha_{dinosterol\text{-}water}$ error bars differ from the analytical uncertainty reported in Table 2. All data with the exception of three fresh/brackish water outliers are used to calculate the bold regression line, and 95% confidence (dark gray solid lines) and prediction bands (dark gray dotted lines). Data are also grouped by sub-region and plotted in color, with regression lines that correspond to the symbol color (see legend). The linear fit for all dinosterol (excluding the outliers) was also assessed using 10,000 iterations in a Monte Carlo (MC) approach in order to incorporate the large, asymmetric and sample-specific uncertainty for many data points (light gray lines). Histograms of the slope and intercept values for each of the MC-regression lines are shown at the right. The table at the bottom lists all slope, intercept, R^2, and P values calculated by standard methods for each regression line shown in the scatter plot, or group of lines for the MC-calculated values. Uncertainty values for the slope, intercept, and R^2 values are standard error, except for the MC uncertainty, which is the standard deviation of all calculated slopes and intercepts, respectively. (For interpretation of the references to colour in this figure legend, the reader is referred to the web version of this article.)

salinity in order to avoid over-representing a single site (both values listed in Table 2).

Dinosterol and brassicasterol α values are correlated with salinity (Figs. 3 and 4; Table 2). Correlation coefficients are similar for both lipids (brassicasterol: $N = 13$; $R^2 = 0.73$, $P = 0.0002$; MC-$R^2 = 0.66$) (dinosterol: $N = 32$; $R^2 = 0.66$, $P = <0.0001$; MC: $R^2 = 0.58$). We have omitted the dinosterol samples from freshwater environments and one brackish site (Table 2 and references therein) from the regression analysis of $\alpha_{dinosterol\text{-}water}$ values and salinity in Fig. 3. The α values from these two freshwater dinosterol samples, one from El Junco Lake in the Galápagos and the other from Great Pond, MA (Sauer et al., 2001), and the brackish Lake Diablo, Galápagos ($S = 7$) are consistent with the fractionations estimated at hypersaline sites (Fig. 3). That so much variability is observed among fresh and low salinity environments indicates that other factors are important in determining the magnitude of D/H fractionation in these locations. These non-salinity driven isotope effects are apparently not common to all brackish sites since the dinosterol α value, from Clipperton Lagoon ($S = 5$) plots in accordance with the α–salinity relationship defined by higher salinity environments.

In addition to the presence of outliers in the α–salinity relationship, $\alpha_{dinosterol\text{-}water}$ values also show more scatter around the regression line than brassicasterol (Figs. 3 and 4). Given the relatively large amount of scatter for both compounds we compared the relationship between α values and salinity for subsets of the data in order to assess the extent to which any relationship might be driven by a low number of samples. This issue is potentially most concerning for dinosterol with fewer samples that approach the salinity of the Great Salt Lake ($S = 117$ ppt) as compared to brassicasterol (Figs. 3 and 4; Table 2).

Dinosterol data from tropical ($N = 7$) and continental ($N = 9$) subsets have α–salinity slopes of 0.0008 and 0.0010, respectively (approximately 0.8‰ and 1‰ per unit change in salinity). These are closer to the published value for the Chesapeake Bay subset ($N = 16$, slope = 0.0010, Fig. 3) (Sachs and Schwab, 2011). Correlations are similar to the whole data set for the tropical ($R^2 = 0.56$) and Chesapeake Bay subsets ($R^2 = 0.57$), and higher for the continental subset ($R^2 = 0.90$). The fact that subset slopes are all greater than the slope from the whole data set implies that despite a strong global salinity effect, region-specific calibrations might be more appropriate for paleoclimate application, and that the sensitivity of α values to salinity might be higher than suggested by the whole data set regression. In either case, the fact that similar relationships are observed between α and salinity for dinosterol in each subset argues against the whole data set regression being driven by only a few high salinity samples.

Although fewer total measurements exist for brassicasterol, the regression lines for the tropical ($N = 4$; slope = 0.0008, intercept = 0.725) and continental ($N = 9$; slope = 0.0007, intercept 0.739) subsets are more similar to each other than are the dinosterol tropical ($N = 7$; slope = 0.0008, intercept = 0.694) and continental ($N = 9$; slope = 0.0010, intercept = 0.665) subsets (Figs. 3 and 4). While this might suggest greater consistency for this compound, more samples are probably required before this conclusion can be made. Explanations for the differences between subsets remain speculative, but for dinosterol at least, these could be related to differences between producers at continental sites from those in more marine-like locations. This possibility is supported by the observation that the Chesapeake Bay and tropical Pacific dinosterol data group more closely on the α–salinity plot as compared to the values from continental sites (Fig. 3). Regardless of these complexities, it is clear at this time that the α–salinity relationships for dinosterol and brassicasterol are not being driven by a few samples or the differences between subsets, but do in fact represent a real environmental signal.

4.3. Potential non-salinity influences on D/H fractionation

The deviation from the α–salinity relationship at some low salinity sites for dinosterol indicates either that alternate factors become dominant in controlling α values at low salinity, or that the magnitude of D/H fractionation during dinosterol synthesis differs between halotolerant species of dinoflagellates and some species with limited or no halotolerance. A similar breakdown of the α–salinity relationship is not observed for brassicasterol from brackish environments (Fig. 4). While it remains possible that a similar non-salinity driven isotope effect occurs in freshwater environments for brassicasterol and that it was simply missed in the smaller sample set, the $\alpha_{brassicasterol\text{-}water}$ value from Lake Diablo provides evidence against this explanation. The $\alpha_{dinosterol\text{-}water}$ value from this brackish site ($S = 7$) is one of the low-salinity outliers in the $\alpha_{dinosterol\text{-}water}$–salinity relationship (Fig. 3). Whatever factors were responsible for driving the anomalous value from this site therefore did not affect the brassicasterol α value. Were this $\alpha_{dinosterol\text{-}water}$ value to reflect variability in other environmental factors like nutrient limitation, growth rate changes or temperature, the brassicasterol-producing diatoms and the dinosterol-producing dinoflagellates might be expected to respond similarly. We consider it more likely that different species of dinosterol producers are found in some low salinity settings and that these organisms fractionate hydrogen isotopes differently than more halotolerant producers. Indeed, different species of cultured green microalgae can have δD values of the same lipid that differ by ~100‰ (Zhang and Sachs, 2007) so similar species effects might also exist for dinoflagellates. Additional field measurements of brassicasterol and dinosterol at lowered salinity ranges combined with species assemblage work will help to define

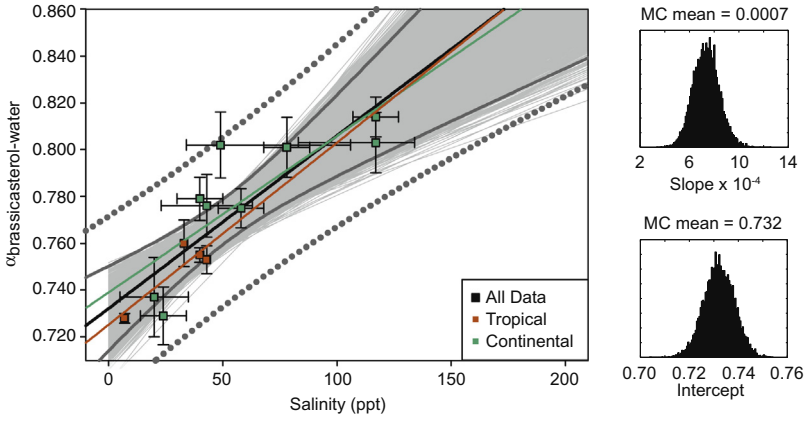

	N	slope	±	intercept	±	R^2	±	P
All Data	**13**	0.0007	0.0001	0.732	0.008	0.732	0.016	0.0002
All Data - MC	**13**	0.0007	0.0001	0.732	0.006	0.656	0.113	-
Tropical	**4**	0.0008	0.0003	0.725	0.009	0.798	0.008	0.1066
Continental	**9**	0.0007	0.0002	0.739	0.013	0.663	0.019	0.0121

Fig. 4. Salinity vs. $\alpha_{brassicasterol\text{-}water}$ (scatter plot). Error bars on each data point incorporate inferred historical changes in salinity and δD_{water} values in addition to the analytical uncertainty from the $\delta D_{brassicasterol}$ measurement (see text). $\alpha_{brassicasterol\text{-}water}$ error bars differ from the analytical uncertainty reported in Table 2. All data with the exception of three fresh/brackish water outliers are used to calculate the bold regression line, and 95% confidence (dark gray solid lines) and prediction bands (dark gray dotted lines). Data are also grouped by sub-region and plotted in color, with regression lines that correspond to the symbol color (see legend). The linear fit for all brassicasterol (excluding the outliers) was also assessed using 10,000 iterations in a Monte Carlo (MC) approach in order to incorporate the large, asymmetric and sample-specific uncertainty for many data points (light gray lines). Histograms of the slope and intercept values for each of the MC-regression lines are shown at the right. The table at the bottom lists all slope, intercept, R^2, and P values calculated by standard methods for each regression line shown in the scatter plot, or group of lines for the MC-calculated values. Uncertainty values for the slope, intercept, and R^2 values are standard error, except for the MC uncertainty, which is the standard deviation of all calculated slopes and intercepts, respectively. (For interpretation of the references to colour in this figure legend, the reader is referred to the web version of this article.)

the variability of low salinity α values at the whole ecosystem export scale.

Another possible cause of the deviation of low-salinity $\alpha_{dinosterol\text{-}water}$ values from those predicted by the $\alpha_{dinosterol\text{-}water}$–salinity relationship observed in sites with more elevated salinity is the potential for heterotrophic dinoflagellates to be more important dinosterol producers in these environments. In some settings dinosterol from heterotrophic dinoflagellates may be a significant contribution to sediments (Amo et al., 2010). The degree to which δD values from heterotrophic organisms reflect any possible climate signal has not been tested as extensively as for lipids from photoautotrophs, but in one case δD values of tetrahymanol, a specific biomarker for heterotrophic bacterivorous ciliates, showed no relationship with climate variability over the past 65 years (Romero-Viana et al., 2013). However, previous applications of dinosterol δD values in environmental and paleoclimate applications have been successful (Sachs et al., 2009; Sachs and Schwab, 2011; Smittenberg et al., 2011). These facts require that either the majority of dinosterol measured in these studies was produced by photoautotrophic dinoflagellates, or that dinosterol δD values from heterotrophic dinoflagellates in these locations are sensitive to environmental variability despite the possible complexities associated with mixed hydrogen sources. Discerning between these two possibilities would be possible with laboratory culture experiments with a variety of heterotrophic and autotrophic dinoflagellates, and species assemblage surveys at these two field sites.

4.4. Comparison of α vs. salinity slopes across diverse environments

The range of α–salinity slopes for the dinosterol and brassicasterol data sets of approximately 0.0007–0.0010 per unit change in salinity, or approximately 0.7–1‰ (Figs. 3 and 4) (Sachs and Schwab, 2011) are similar to those found for a variety of cyanobacterial and algal lipids from hypersaline ponds on Christmas Island (Sachse and Sachs, 2008) (Fig. 5). Although the slopes of the relationships from the Chesapeake Bay (Sachs and Schwab, 2011) and Christmas Island (Sachse and Sachs, 2008) are slightly different in some cases from the results identified in the current study, some of this may be due to the scatter in our data owing to the uncertainty in salinity and δD_{water} changes over the time, as well as the inherent variability in all field data due to factors such as variable growth rates, species assemblages, and temperatures. We also note that the Chesapeake Bay study referenced the measured dinosterol δD values to the VSMOW scale using co-injection standards within the Isodat software package. By definition this is only a one-point calibration (Ricci et al., 1994), and therefore fails to take into account the possibility of any scale stretching or compression, which can produce systematic biases in measured δD values (Coplan, 1988; Meier-Augenstein et al., 2013). Conversely, our data were post-processed to ensure no scale stretch or compression was present that could result in slight biasing the slope and intercept of an α–salinity regression. These minor differences in referencing strategies may therefore account for some component of the apparent disagreement between the different data sets.

In contrast to the general consistency among the α–salinity slopes for dinosterol and brassicasterol with Christmas Island lipids is the lack of any discernible dependence of D/H fractionation in alkenones on salinity from sites in the present study where these compounds were found (Nelson and Sachs, 2014) as well as from the Chesapeake Bay (Schwab and Sachs, 2011). These results are also in contrast to results from batch culture experiments using marine haptophytes, which implied a much steeper relationship for alkenones of approximately 0.003 α units per unit change in salinity (Schouten et al., 2006), although this slope may have been amplified due to a growth rate effect (c.f. Zhang et al., 2009). Previous interpretations of the alkenone α–salinity calibrations postulated that the discrepancy between the batch culture and field experiments was related to the difference between marine and coastal/lacustrine producers (Schwab and Sachs, 2011; Nelson and Sachs, 2014). That dinosterol and brassicasterol α values from diverse field settings do show a relationship with salinity further substantiates this conclusion, and highlights the possibility of unique halotolerance mechanisms for lacustrine alkenone producers. These observations warrant a more targeted study with culture experiments of lacustrine alkenone producers.

5. CONCLUSION

We have evaluated the extent to which salinity is a dominant control on the magnitude of D/H fractionation in algal lipids through measurements of dinosterol and brassicasterol $\alpha_{lipid\text{-}water}$ values over a diverse range of lake and lagoon systems. Our results demonstrate that D/H fractionation decreases as salinity increases for dinosterol and brassicasterol in virtually all locations, consistent with patterns identified previously from algal lipids grown in batch culture (Schouten et al., 2006), and from single-location field studies in the Chesapeake Bay (Sachs and Schwab, 2011) and hypersaline ponds on Christmas Island (Sachse and Sachs, 2008). For reasons we do not yet understand, fractionation factors in the limited number of freshwater systems we investigated are not consistent with the zero salinity intercept value predicted by the saline systems However, since the same lipid produced by different species of green microalgae cultured in the same media can have δD values that differ by 100‰ (Zhang and Sachs, 2007) this is perhaps not surprising.

The agreement between our global-scale results and previously published algal lipid α–salinity relationships significantly strengthens the case for salinity as the dominant factor responsible for modulating D/H fractionation in biosynthesis of many algal lipids in saline and hypersaline environments. Although other factors are certainly relevant and are a likely explanation for why we do not observe R^2 values greater than 0.6–0.9 for linear regressions of $\alpha_{lipid\text{-}water}$ on salinity, our results offer strong support for interpretation of algal lipid δD values as a function of both changing salinity and water δD values with a magnitude of 0.7–1‰ per unit change in salinity. The apparent consistency of this

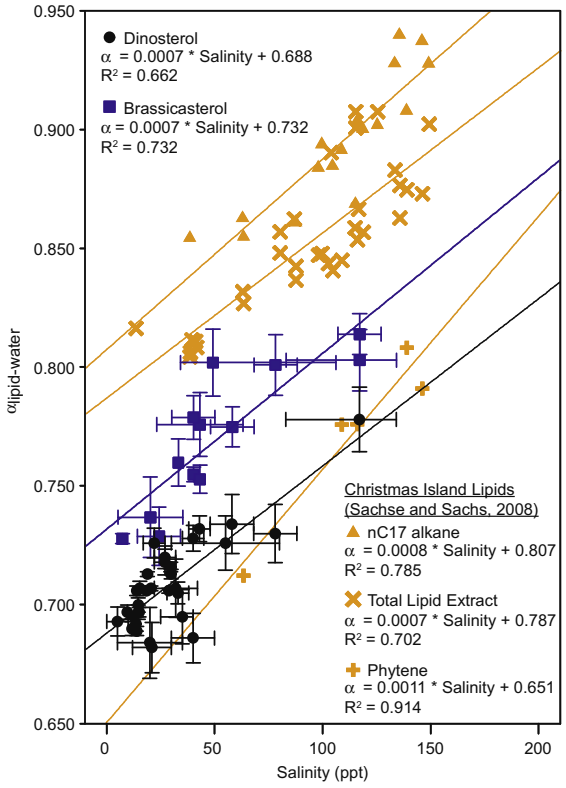

Fig. 5. Comparison of $\alpha_{lipid\text{-}water}$ vs. salinity data for dinosterol and brassicasterol with data from hypersaline ponds on Christmas Island (Sachse and Sachs, 2008). Note the color change for brassicasterol from Fig. 4. Non-Monte Carlo regression lines for dinosterol and brassicasterol are repeated from the whole data set from Figs. 3 and 4. Christmas Island regressions statistics are not shown here (see Sachse and Sachs, 2008). (For interpretation of the references to colour in this figure legend, the reader is referred to the web version of this article.)

relationship across diverse environments supports the application of dinosterol or brassicasterol measurements from sediment cores as a powerful new tool for reconstructing paleosalinity in lakes. This application may also be enhanced to produce quantitative reconstructions of lake water δD values and salinity when dinosterol or brassicasterol δD values are combined with additional isotopic proxy data such as δD values from a second biomarker, or the oxygen isotopic composition of lacustrine carbonate.

Monte Carlo regression analyses (Figs. 3 and 4) demonstrate that the maximum possible α–salinity relationship that can be supported by the brassicasterol and dinosterol data is no more than 0.0012 per unit change in salinity. These results are consistent with results from cyanobacterial and algal lipids from Christmas Island and the Chesapeake Bay, which showed fractionation factors as a function of salinity in the range of 0.0007–0.0011 (Sachse and Sachs, 2008; Sachs and Schwab, 2011). These all demonstrate a much lower sensitivity of D/H fractionation to salinity than the 0.003 per unit change in salinity reported for alkenones from coccolithophorid batch culture experiments (Schouten et al., 2006). Given the relative importance of alkenones for paleoclimate applications it would be valuable to assess this α–salinity sensitivity using chemostat-type experiments, which would allow for growth rates to be maintained at constant levels.

Without targeted mechanistic studies under controlled laboratory conditions we can offer no additional insight on the underlying mechanism to cause the observed salinity modulation of D/H fractionation beyond those discussed in previous calibration studies of dinosterol (e.g. Sachs and Schwab, 2011). While such laboratory experiments would be informative for improved understanding of lipid biosynthesis processes and species distributions, they might only be justified from the perspective of paleoclimate proxy development after the sensitivity of dinosterol to environmental variability has been evaluated over a larger range of environments, which has been a primary outcome of our study. Our results contribute to a more complete characterization of the degree and magnitude to which environmental factors act to influence the magnitude of D/H fractionation in algal lipid synthesis. Continued advancement of this research area will enable more confident and quantitative applications of lipid δD values to reconstruct past climate variability.

ACKNOWLEDGMENTS

This material is based upon work supported by the U.S. National Science Foundation under Grants NSF-EAR-0745982, EAR-0823503 and ESH-0639640, and the U.S. National Oceanic and Atmospheric Administration under Grant No. NA08OAR4310685 to J. Sachs. The authors would like to thank Alyssa Atwood, Ines Mugler, and Julie Richey for providing surface sediment dinosterol δD values. We thank Hedi Oberhänsli for providing samples from the Aral Sea, and Robert Baskin for providing samples from the Salton Sea. We thank Orest Kawka, Josh Gregersen, S. Nemiah Ladd, Alyssa Atwood, Ines Mügler, and Julie Richey for useful discussions, advice and assistance in the lab. We thank Ariel Townsend for her careful assistance in the lab. We thank Jeff Bowman, Alyssa Atwood, Simon Haberle, S. Nemiah Ladd, Olivier Cartapanis, Fran Janny, and Conor Myhrvold for assistance in the field. We thank Associate Editor Alex Sessions and three anonymous reviewers for their comments, which greatly improved the quality of this manuscript.

APPENDIX A. SUPPLEMENTARY DATA

Supplementary data associated with this article can be found, in the online version, at http://dx.doi.org/10.1016/j.gca.2014.03.007.

REFERENCES

Amo M., Suzuki N., Kawamura H., Yamaguchi A., Takano Y. and Horiguchi T. (2010) Sterol composition of dinoflagellates: different abundance and composition in heterotrophic species and resting cysts. *Geochem. J.* **44**, 225–231.

Anati D. A. (1999) The salinity of hypersaline brines: concepts and misconceptions. *Int. J. Salt Lake Res.* **8**, 55–70.

Arnow T. and Stephens D. (1990) *Hydrologic Characteristics of the Great Salt Lake, Utah: 1847–1986, United States Geological Survey Water-Supply*. U.S. Geological Survey.

Atwood A. R. and Sachs J. P. (2012) Purification of dinosterol from complex mixtures of sedimentary lipids for hydrogen isotope analysis. *Org. Geochem.* **48**, 37–46.

Benson L. and Paillet F. (2002) HIBAL: a hydrologic-isotopic-balance model for application to paleolake systems. *Quatern. Sci. Rev.* **21**, 1521–1539.

Bowman J. S. and Sachs J. P. (2008) Chemical and physical properties of some saline lakes in Alberta and Saskatchewan. *Saline Systems* **4**, 3. http://dx.doi.org/10.1186/1746-1448-4-3.

Coplan T. B. (1988) Normalization of oxygen and hydrogen isotope data. *Chem. Geol. (Isotope Geosci. Sect.)* **72**, 293–297.

Craig H. (1961) Isotopic variations in meteoric waters. *Science* **133**, 1702–1703.

Craig H. and Gordon L. I. (1965). In *Proceedings of a Conference on Stable Isotopes in Oceanographic Studies and Paleotemperatures* (ed. E. Tongiori). CNR-Laboratorio di Geologia Nucleare, Pisa, pp. 9–130.

Douglas P. M. J., Pagani M., Brenner M., Hodell D. A. and Curtis J. H. (2012) Aridity and vegetation composition are important determinants of leaf-wax dD values in southeastern Mexico and Central America. *Geochim. Cosmochim. Acta* **97**, 24–45.

Fofonoff N. P. (1985) Physical properties of seawater: a new salinity scale and equation of state for seawater. *J. Geophys. Res.* **90**, 3332–3342.

Hammer U. T. (1978) The Saline Lakes of Saskatchewan III. Chemical Characterization. *Int. Rev. Gesamten Hydrobiol. Hydrograph.* **63**, 311–335.

Hou J., D'Andrea W. J. and Huang Y. (2008) Can sedimentary leaf waxes record D/H ratios of continental precipitation? Field, model, and experimental assessments. *Geochim. Cosmochim. Acta* **72**, 3503–3517.

Kahmen A., Schefuß E. and Sachse D. (2013) Leaf water deuterium enrichment shapes leaf wax n-alkane δD values of angiosperm plants I: experimental evidence and mechanistic insights. *Geochim. Cosmochim. Acta* **111**, 39–49.

Ladd S. N. and Sachs J. P. (2012) Inverse relationship between salinity and n-alkane δD values in the mangrove *Avicennia marina*. *Org. Geochem.* **48**, 25–36.

Liu W. and Yang H. (2008) Multiple controls for the variability of hydrogen isotopic compositions in higher plant n-alkanes from modern ecosystems. *Global Change Biol.* **14**, 2166–2177.

McInerney F. A., Helliker B. R. and Freeman K. H. (2011) Hydrogen isotope ratios of leaf wax n-alkanes in grasses are insensitive to transpiration. *Geochim. Cosmochim. Acta* **75**, 541–554.

Meier-Augenstein W., Hobson K. A. and Wassenaar L. I. (2013) Critique: measuring hydrogen stable isotope abundance of proteins to infer origins of wildlife, food and people. *Bioanalysis* **5**, 751–767.

Micklin P. (2007) The Aral Sea disaster. *Annu. Rev. Earth Planet. Sci.* **35**, 47–72.

Nelson D. B. and Sachs J. P. (2013) Concurrent purification of sterols, triterpenols and alkenones from sediments for hydrogen isotope analysis using high performance liquid chromatography. *Org. Geochem.* **64**, 19–28.

Nelson D. B. and Sachs J. P. (2014) The influence of salinity on D/H fractionation in alkenones from saline and hypersaline lakes in continental North America. *Org. Geochem.* **66**, 38–47.

Nelson D. B., Abbott M. B., Steinman B., Polissar P. J., Stansell N. D., Ortiz J. D., Rosenmeier M. F., Finney B. P. and Riedel J. (2011) Drought variability in the Pacific Northwest from a 6000-yr lake sediment record. *Proc. Natl. Acad. Sci. U.S.A.* **108**, 3870–3875.

Nelson D. M., Henderson A. K., Huang Y. and Hu F. S. (2013) Influence of terrestrial vegetation on leaf wax dD of Holocene lake sediments. *Org. Geochem.* **56**, 106–110.

Nielson K. E. and Bowen G. J. (2010) Hydrogen and oxygen in brine shimp chitin reflect environmental water and dietary isotopic composition. *Geochim. Cosmochim. Acta* **74**, 1812–1822.

Nourgaliev D. K., Heller F., Borisov A. S., Hajdas I., Bonani G., Iassonov P. G. and Oberhänsli H. (2003) Very high resolution paleosecular variation record for the last 1200 years from the Aral Sea. *Geophys. Res. Lett.*, 30.

Polissar P. J. and Freeman K. H. (2010) Effects of aridity and vegetation on plant-wax δD in modern lake sediments. *Geochim. Cosmochim. Acta* **74**, 5785–5797.

Polissar P. J., Freeman K. H., Rowley D. B., McInerney F. A. and Currie B. S. (2009) Paleoaltimetry of the Tibetan Plateau from D/H ratios of lipid biomarkers. *Earth Planet. Sci. Lett.* **287**, 64–76.

Rampen S. W., Abbas B. A., Schouten S. and Sinninghe-Damsté J. S. (2010) A comprehensive study of sterols in marine diatoms (Bacillariophyta): implications for their use as tracers for diatom productivity. *Limnol. Oceanogr.* **55**, 91–105.

Ricci M. P., Merritt D. A., Freeman K. and Hayes J. M. (1994) Acquisition and processing of data for isotope-ratio-monitoring mass spectrometry. *Org. Geochem.* **21**, 561–571.

Romero-Viana L., Kienel U., Wilkes H. and Sachse D. (2013) Growth-dependent hydrogen isotopic fractionation of algal lipid biomarkers in hypersaline Isabel Lake (Mexico). *Geochim. Cosmochim. Acta* **106**, 490–500.

Rozanski K., Araguás-Araguás L. and Gonfiantini R. (1992) Relation between long-term trends of oxygen-18 isotope composition of precipitation and climate. *Science* **258**, 981–985.

Sachs J. P. and Schwab V. F. (2011) Hydrogen isotopes in dinosterol from the Chesapeake Bay estuary. *Geochim. Cosmochim. Acta A* **75**, 444–459.

Sachs J. P., Sachse D., Smittenberg R. H., Zhang Z., Battisti D. S. and Golubic S. (2009) Southward movement of the Pacific intertropical convergence zone AD 1400–1850. *Nat. Geosci.* **2**, 519–525.

Sachse D. and Sachs J. P. (2008) Inverse relationship between D/H fractionation in cyanobacterial lipids and salinity in Christmas Island saline ponds. *Geochim. Cosmochim. Acta* **72**, 793–806.

Sachse D., Kahmen A. and Gleixner G. (2009) Significant seasonal variation in the hydrogen isotopic composition of leaf-wax lipids for two deciduous tree ecosystems (*Fagus sylvativa* and *Acer pseudoplatanus*). *Org. Geochem.* **40**, 732–742.

Sachse D., Billault I., Bowen G. J., Chikaraishi Y., Dawson T. E., Feakins S. J., Freeman K. H., Magill C. R., McInerney F. A., van der Meer M. T. J., Polissar P., Robins R. J., Sachs J. P., Schmidt H.-L., Sessions A. L., White J. W. C., West J. B. and Kahmen A. (2012) Molecular paleohydrology: interpreting the hydrogen-isotopic composition of lipid biomarkers from photosynthesizing organisms. *Annu. Rev. Earth Planet. Sci.*, 40.

Sauer P. E., Eglinton T. I., Hayes J. M., Schimmelmann A. and Sessions A. L. (2001) Compound-specific D/H ratios of lipid biomarkers from sediments as a proxy for environmental and climatic conditions. *Geochim. Cosmochim. Acta* **65**, 213–222.

Schouten S., Ossebaar J., Schreiber K., Kienhuis M. V. M., Langer G., Benthien A. and Bijma J. (2006) The effect of temperature, salinity and growth rate on the stable hydrogen isotopic composition of long chain alkenones produced by *Emiliania huxleyi* and *Gephyrocapsa oceanica*. *Biogeosciences* **3**, 113–119.

Schroeder R. A., Orem W. H. and Kharaka Y. K. (2002) Chemical evolution of the Salton Sea, California: nutrient and selenium dynamics. *Hydrobiologia* **473**, 23–45.

Schwab V. F. and Sachs J. P. (2011) Hydrogen isotopes in individual alkenones from the Chesapeake Bay estuary. *Geochim. Cosmochim. Acta* **75**, 7552–7565.

Sessions A. L., Burgoyne T. W. and Hayes J. M. (2001) Determination of the H3 Factor in hydrogen isotope ratio monitoring mass spectrometry. *Anal. Chem.* **73**, 200–207.

Smith F. A. and Freeman K. H. (2006) Influence of physiology and climate on delta D of leaf wax n-alkanes from C-3 and C-4 grasses. *Geochim. Cosmochim. Acta* **70**, 1172–1187.

Smittenberg R. H., Saenger C., Dawson M. N. and Sachs J. P. (2011) Compound-specific D/H ratios of the marine lakes of Palau as proxies for West Pacific Warm Pool hydrologic variability. *Quatern. Sci. Rev.* **30**, 921–933.

Steinman B., Abbott M. B., Mann M. E., Stansell N. D. and Finney B. P. (2012) 1500 year quantitative reconstruction of winter precipitation in the Pacific Northwest. *Proc. Natl. Acad. Sci. U.S.A.* **109**, 11619–11623.

Tipple B. J., Berke M. A., Doman C. E., Khachaturyan S. and Ehleringer J. R. (2013) Leaf-wax n-alkanes record the plant–water environment at leaf flush. *Proc. Natl. Acad. Sci. U.S.A.* **110**, 2659–2664.

USGS (2013) *Great Salt Lake – Salinity and Water Quality*. Utah Water Science Center, U.S. Department of the Interior (http://ut.water.usgs.gov/greatsaltlake/salinity/index.html).

van der Meer M. T. J., Benthien A., Bijma J., Schouten S. and Sinninghe-Damsté J. S. (2013) Alkenone distribution impacts the hydrogen isotopic composition of the C37:2 and C37:3 alkan-2-ones in *Emiliania huxleyi*. *Geochim. Cosmochim. Acta* **111**, 162–166.

Vance R. E., Clague J. J. and Mathewes R. W. (1993) Holocene Paleohydrology of a hypersaline lake in southeastern Alberta. *J. Paleolimnol.* **8**, 103–120.

Volkman J. K. (2003) Sterols in microorganisms. *Appl. Microbiol. Biotechnol.* **60**, 495–506.

Volkman J. K., Barrett S. M., Blackburn S. I., Mansour M. P., Sikes E. L. and Gelin F. (1998) Microalgal biomarkers: s review of recent research developments. *Org. Geochem.* **29**, 1163–1179.

Wolhowe M. D., Prahl F. G., Probert I. and Maldonado M. (2009) Growth phase dependent hydrogen isotopic fractionation in alkenone-producing haptophytes. *Biogeosciences* **6**, 1681–1694.

Yang H., Pagani M., Briggs D. E. G., Equiza M. A., Jagels R., Leng Q. and LePage B. A. (2009) Carbon and hydrogen isotope fractionation under continuous light: implications for paleoenvironmental interpretations of the High Arctic during Paleogene warming. *Oecologia* **160**, 461–470.

Zarrouk W., Carrasco-Pancorbo A., Zarrouk M., Segura-Carretero A. and Fernández-Gutiérrez A. (2009) Multi-component analysis (sterols, tocopherols and triterpenic dialcohols) of the unsaponifiable fraction of vegetable oils by liquid chromatography–atmospheric pressure chemical ionization–ion trap mass spectrometry. *Talanta* **80**, 924–934.

Zhang Z. and Sachs J. P. (2007) Hydrogen isotope fractionation in freshwater algae: I. Variations among lipids and species. *Org. Geochem.* **38**, 582–608.

Zhang Z., Sachs J. P. and Marchetti A. (2009) Hydrogen isotope fractionation in freshwater and marine algae: II. Temperature and nitrogen limited growth rate effects. *Org. Geochem.* **40**, 428–439.

Zhou Y., Grice K., Chikaraishi Y., Stuart-Williams H., Farquhar G. D. and Ohkouchi N. (2011) Temperature effect on leaf water deuterium enrichment and isotopic fractionation during leaf lipid biosynthesis: Results from controlled growth of C3 and C4 land plants. *Phytochemistry* **72**, 207–213.

Associate editor: Alex L. Sessions